J. Phys. IV France **11** (2001)

Nanoscale inhomogeneities in melt-spun Ni-Al

P.L. Potapov, P. Ochin[1], J. Pons[2] and D. Schryvers

Electron Microscopy for Materials Research (EMAT), University of Antwerp, RUCA, Groenenborgerlaan 171, 2020 Antwerp, Belgium
[1] *Laboratoire de Métallurgie Structurale, ENSCP, 11 rue Pierre et Marie Curie, 75231 Paris cedex 05, France*
[2] *Departament de Física, Universitat de les Illes Balears, Ctra. de Valldemossa km 7.5, 07071 Palma de Mallorca, Spain*

Abstract. Ni-Al material consisting 62 ...65%Ni was rapidly quenched to room temperature by the melt-spinning technique and studied using X-ray diffraction, different transmission electron microscopy (TEM) modes and calorimetry measurements. Similar to bulk material, the initial B2 structure undergoes a martensitic transformation to the L1o or 14M structure. However, the transformation proceeds very inhomogeneously and results in a mixed microstructure consisting of transformed and untransformed regions. The structure of the transformed regions varies from faulted L1o to faulted 14M and shows a variety of morphological features. EDX and EELS nanoprobes reveal that the special structural state of the melt-spun material is explained mainly by solute segregation appearing during the crystallisation process. Thus, contrary to most of other melt quenched materials, in Ni-Al, solute segregation can not be suppressed by the rapid quenching procedure. Ageing at 1200^{0}C restores the compositional homogeneity and results in more homogenious martensitic transformation resembling that in bulk Ni-Al material.

1. INTRODUCTION

The Ni-Al intermetallic compound in the composition range from 42 to 70 at.%Ni attracts much attention due to the unique combination of a high melting point, a low density and a high oxidation resistance. Like many other B2 compounds, Ni-rich Ni-Al (with about 62-69 at.% Ni) undergoes a diffusionless {110}<110> martensitic shear transformation on cooling resulting in a multiply twinned tetragonal $L1_0$ structure [1-4]. On heating, the B2 structure is restored by the reverse shear. In compositions with less than 63 at.% Ni, the low temperature structure is more complicated and can be described as $L1_0$ with periodical microtwins on 111_{L1_0} planes [5,6]. This structure typically has a stacking period of 7 layers with a $(5\bar{2})$ sequence and is denoted as 14M [7] (formerly referred to as 7R or 7M). Occasionally, other stacking sequences, such as a 10 layered stacking have been observed [8]. Whether or not the 14M structure should be considered as an independent structure or simply a variation of $L1_0$ with fine twins accommodating the transformation strain, is still a matter of discussion [8-10]. Still, as most reports on Ni-Al refer to the $(5\bar{2})$ stacking, the 14M structure will be used as the reference case for the long period martensite in the present discussions.

These days advanced preparation techniques involving the direct quench from the melt with a cooling rate up to 10^6 K/s are readily available. However, the first studies of rapidly quenched Ni-Al revealed a more complicated structural situation than that in conventional (bulk) material. Kennon et al. [11] found the 14M structure mixed with $L1_0$ in melt-spun $Ni_{66}Al_{34}$ ribbons although 14M is never observed in bulk material with such a high Ni content. Chandrasekaran et al. [12] reported that the stacking sequence of the martensitic phase varies from 7 to 10 close packed layers in splat-cooled Ni-Al material. Schryvers & Holland-Moritz [13] pointed out an unusual variety of morphologies of the $L1_0$ and 14M structure and also the occasional appearance of the B2 structure in Ni-rich compositions, and opposite, the appearance of $L1_0$ in Ni-poor compositions of splat-cooled Ni-Al being normally mono-structural B2 in bulk material. Thus, some unknown factors related with the rapid quench procedure seem to strongly affect the structural state of Ni-Al alloys.

This paper analyses the transformation behaviour in rapidly quenched Ni-Al material in comparison with that in conventional bulk material. Although only one representative example of melt-spun $Ni_{65}Al_{35}$ ribbons is described below, similar results were obtained in $Ni_{62.5}Al_{37.5}$ composition [14]. New information on the structural state and transformation behaviour of rapidly quenched Ni-Al ribbons are discussed in terms of nanoscale composition inhomogeneities formed during the quenching procedure.

2. EXPERIMENTAL

Melt-spun Ni-Al ribbons containing 65 at.% of Ni, henceforth referred to as 65Ni, were manufactured by the single-roller melt-spinning technique, which yielded a cooling rate between 10^5 and 10^6K/s [15]. As a reference for comparison of properties between the bulk and spun materials, bulk 63.8Ni material prepared by powder metallurgy was used. Some of ribbons were evacuated in quartz tubes and annealed at 1200°C for 20 min. followed by water quenching with breaking the tubes.

DSC measurements were executed in the range from –120°C to +400°C with a rate of 20K/min for rough determination of the transformation interval and with a rate of 3K/min for careful measurement of transformation heat effects in the range of interest. Measurements were performed after 2 thermocycles between –70°C to +150°C. Before the first heating, samples were cooled down to -70°C without recording the curve. X-ray diffraction studies were performed in the θ-2θ mode using a powder Philips PW1830 diffractometer with a monochromated Cu K_α radiation. The conventional TEM and analytical studies were performed on a Philips CM20-twin microscope equipped with a Si(Li) Oxford EDX detector and on a Philips CM30 field emission microscope equipped with a Gatan electron energy loss spectroscopy (EELS) detector. The high resolution transmission electron microscopy (HRTEM) images were obtained with a JEOL 4000 EX microscope equipped with a top-entry stage.

3. RESULTS

Fig.1 displays X-ray scans of 65Ni in the as-spun and annealed state. As-spun 65Ni shows overlapping diffraction patterns of three structures: B2, $L1_0$ and 14M. Following the crystallography of the B2→$L1_0$ and B2→14M martensitic transformations, the transformed structures are coherent with the parent B2 structure and the $<111>_{L1_0}$ and $<1\bar{1}7>_{14M}$ directions are close to the <110> directions of B2. Therefore, when only these lines are considered, their relative intensities can be used for a simple quantitative analysis of the volume fractions of the phases involved. The analysis of the line intensities in Table 1 reveals an occupancy of 30%, 25% and 45% for the B2, $L1_0$ and 14M structures, respectively. Thus, the B2→$L1_0$ (14M) transformation is incomplete at room temperature and the material is being frozen in a stage in which the initial and transformed structures coexist with each other. Annealed 65Ni shows the single B2 X-ray pattern, which indicates that the transformation proceeds below room temperature.

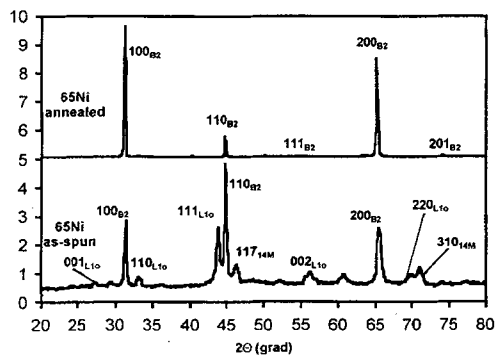

Figure 1 X-ray diffraction scans of as-spun and annealed 65Ni.

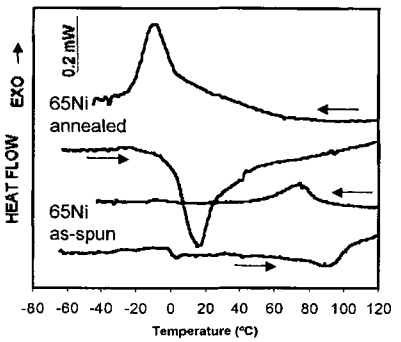

Figure 2 DSC curves of as-spun and annealed 65Ni on heating and cooling with a rate of 3K/min.

Differential scanning calorimetry (DSC) measurements demonstrate that the transformation in as-spun 65Ni proceeds in an unusual way. As the preliminary scanning between –70°C and +400°C only revealed peaks in the 0°C ...+120°C temperature range, the slow scanning, i.e. at a rate of 3K/min, was undertaken between –70°C and +120°C. The DSC curve of as-spun 65Ni in Fig.2 shows one doublet of endo- and exothermic peaks around 80°C upon heating and cooling, respectively, with a hysteresis of 20°C. The latter is consistent with the transition between B2 and $L1_0$ in bulk material, which is reversible and

exhibits a hysteresis of 10-25°C [16,17]. As a confirmation, the hysteresis in the reference bulk 63.8Ni sample was found to be 18°C. However, the 65Ni peaks show a much smaller latent heat of 1.7J/g than the 10.2J/g associated with the complete B2->$L1_0$ transformation in the reference 63.8Ni bulk sample. Coming back to X-ray results, which detected that 70% of material is already transformed at room temperature, we can conclude that most of the transformation proceeds by small undetectable portions over the wide temperature range. Therefore, the peaks observed in Fig.2 are associated with only one portion detectable by DSC (about 20% of the entire transformation). In contrast, annealed 65Ni ribbons demonstrate the transformation localised in the narrow temperature range. The transformation latent heat was measured as 6.4 J/g, which was comparable with that observed in the reference bulk material. At the same time, the transformation temperature in annealed 65Ni is lower than that expected for their nominal composition, which could be explained by Ni depletion during annealing.

Table 1 Volume fractions of the B2, $L1_0$ and 14M structures calculated from the relative intensity of 110_{B2},111_{L1O} and $1\bar{1}7_{14M}$ lines.

Structure	Line index	2θ position (grad)	Experimental integral intensity (counts)	Ni mean scattering factor	Structure factor	Mulipl icity factor	Polycrystal geometrical factor	Lorentz-polarization factor	Calculated volume fraction (%)
B2	110	44.8	2591	14.15	1	12	2.62	3.91	29.8
$L1_0$	111	43.8	1501	14.32	1	8	2.68	4.03	24.2
14M	$1\bar{1}7$*	46.2	588	13.92	0.48**	4	2.55	3.76	46.0

* $1\bar{1}4$ in 7R notations

**calculated from the atomic positions suggested by Martynov et al.[6].

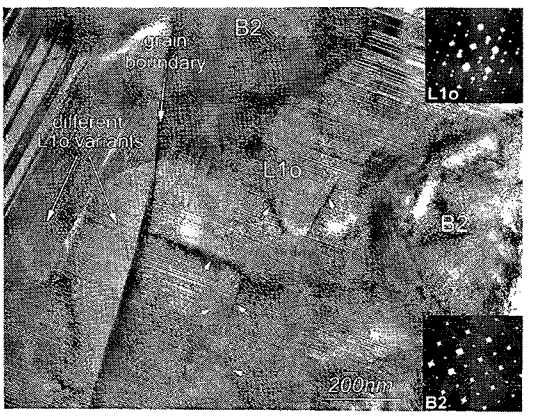

Figure 3 (a) BF [100]$_{B2}$ zone image of 65Ni showing the B2+$L1_0$ mixture with corresponding SAED patterns (dislocations parallel to <211>$_{L1o}$ or <111>$_{L1o}$ are marked by arrows).

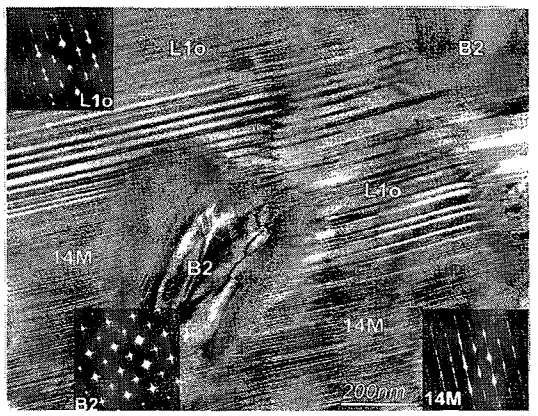

Figure 4 BF [100]$_{B2}$ zone image of 65Ni showing a typical B2+14M+$L1_0$ mixture. The SAED patterns for each structure are shown as insets.

Fig.3 shows the typical microstructure of as-spun 65Ni material observed by TEM at room temperature. Most of the material is transformed into the martensite phase as confirmed by SAED. Still, several untransformed B2 regions with a typical lateral size of 300nm are present. Untransformed B2 regions occupy approximately 1/4 of the entire 65Ni material, which is in good agreement with the X-ray data. The SAED examination reveals that the B2 parts distributed over a large area of the sample have an identical crystallographic orientation, indicating a common crystallographic origin. Near the Bragg positions, strong <110>$_{B2}$ diffuse streaks are observed indicating that the B2 regions are in the precursor state with respect to the {110} <110>$_{B2}$ shear transformation [18,19]. The $L1_0$ regions show the internally

twinned morphology typical for Ni-Al martensite plates, built by combination of two martensite variants separated by $\{111\}_{L1_0}$ twinning planes. Close examination of the SAED patterns reveals a faint diffuse streaking along $<111>_{L1_0}$ indicating the presence of multiple aperiodical $\{111\}<110>_{L1_0}$ stacking defects, in this case resulting in varying twin widths. Sometimes dislocations, mostly parallel to $<211>_{L1_0}$ or $<111>_{L1_0}$ are observed in the $L1_0$ matrix (see Fig.3).

The 14M structure exhibits a similar twinned morphology although the 14M twins are in principle periodic and much finer than the $L1_0$ ones. A perfect 14M structure shows a row of six fine superreflections along the former $<111>_{L1_0}$ directions in reciprocal space, which indicates the formation of periodically arranged $\{111\}$ $<110>_{L1_0}$ microtwin planes. In contrast to the strictly periodical 7 layered structure, observed in bulk material by Martynov et al. [6], the long period martensite in melt-spun 65Ni shows a periodicity varying between 7 and 10 layers which confirms an earlier report by Chandrasekaran et al. [12]. As a rule, this finely twinned long period structure appears nearby the untransformed B2 regions, sometimes forming an intermediate layer between the $L1_0$ and B2 structures. As shown in Fig.4, close to the 14M regions, the $L1_0$ SAED patterns typically exhibit a more pronounced streaking than in the central areas of the martensite plates, indicating more varying twin widths. As seen from Fig.4, the $L1_0$ and 14M structures can replace each other smoothly without changing the microtwin plane.

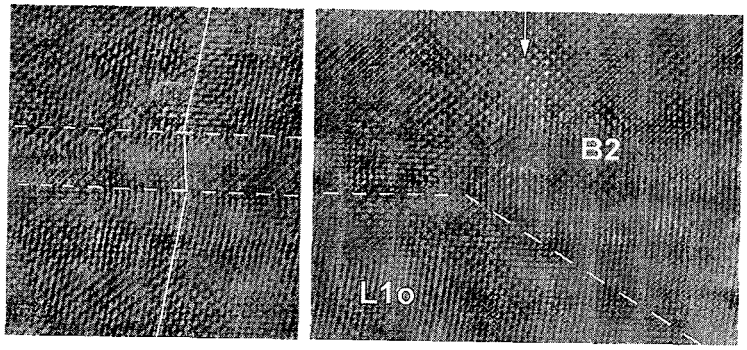

Figure 5 $[100]_{B2}$ HRTEM image of the fine twinned $L1_0$ crystal (left) and the tip of this crystal surrounded by the B2 region (right). Near the interface, a gradual lattice distortion is observed.

As the martensitic transformation is known to proceed by a displacive transformation mechanism, a sharp habit plane is normally observed between the parent and transformed structures. As seen from Fig. 3, conventional TEM images of interfaces between B2 and martensite in spun 65Ni are blurred usually indicating an inclined or less sharp interface. HRTEM indeed shows a gradual lattice distortion over such an interface. Fig.5 displays two HRTEM images observed nearby the B2-$L1_0$ interface. The left image shows the internally twinned martensitic crystal with the dashed lines locating the microtwin planes and the solid, parallel with the trace of a $\{211\}$ type plane, revealing the twinning. The right image shows the tip of the same martensitic crystal surrounded by the B2 area. The interface is roughly located on the dashed line. When looking along a grazing incidence in the direction of the arrow, a region of a few nm around the interface is seen to accommodate the lattice distortion by gradual displacements of the atoms.

In order to investigate the local composition, melt-spun material was examined by precise EDX analysis. In the Ni-Al system, the strong absorption of X-rays generated by the Al atoms is known, thus the special absorption correction after Horita et al.[20] was made. The Cliff-Lorimer factor relating the measured and truth intensity ratio between Ni K_α and Al K_α generated X-rays was measured in the homogeneous 63.8Ni bulk reference sample and then interpolated by a logarithmic curve as a function of the sample thickness and used for calibration of EDX measurements in the melt-spun material [20]. This gives an absolute precision of 1.5 at.% and a relative one, i.e. when comparing two adjacent regions, of 1 at.%. Fig. 6 shows the results of EDX probes at and near a retained B2 region in as-spun 65Ni. The B2 region is characterised by a Ni depleted area of about 600nm in diameter. More such regions were examined always indicating similar results. Although EDX analysis intrinsically implies a random error of ±0.5 at.%, the present extensive statistics allows one to conclude that the B2 regions in 65Ni contain on average 1-3at.% less Ni than the $L1_0$ (14M) matrix.

An additional proof of these concentration inhomogeneities is provided by EELS analysis. As reported several times, the Ni L_3 absorption peak in Ni-Al alloys is split into two sub-peaks and the intensity ratio

between them is composition dependent [21,22]. The second sub-peak is almost absent in pure Ni and rises strongly with increasing Al content due to hybridisation between Ni *d* and Al *s* shells. Fig.7 shows EELS spectra collected from nearby $L1_0$ and B2 regions in as-spun 65Ni. The splitting of L_3 is well resolved and, indeed, the second sub-peak is always slightly lower in $L1_0$ regions as compared to B2 one. This indicates a higher Ni content in the former, corresponding with higher transformation temperatures.

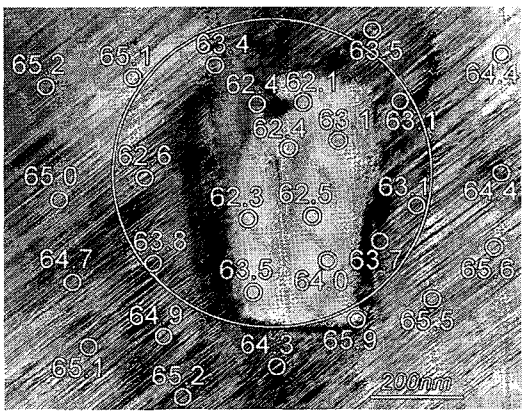

Figure 6 BF images of a B2 region surrounded by 14M and $L1_0$ regions in 65Ni. Small circles and numbers show the probe locations and the EDX measured Ni content. Big circle outlines areas depleted by Ni.

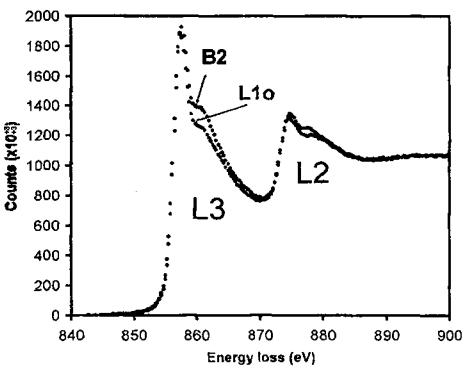

Figure 7 Ni $L_{3,2}$ edges (after deconvolution and background subtraction) of the B2 and $L1_0$ regions in 65Ni The L_3 peak is split into two sub-peaks and the relative intensity of the second sub-peak is a measure of the Al content in the probed region.

4. DISCUSSION

An immediate conclusion from the above presented results is that the transformation of the initial B2 structure into the $L1_0$ or 14M martensite ones proceeds very inhomogeneously in Ni-Al melt-spun material. The local transformation temperature varies from region to region causing the spreading of the entire transformation over the wide temperature range. Also the structure of the transformed areas varies spatially from $L1_0$ to 14M showing a variety of morphologies and features like curvature of twin planes. This conclusion is consistent with earlier observations of rapidly quenched Ni-Al alloys [11-13]. As follows from the presented results such inhomogeneous behaviour is explained mainly by the fine scale compositional inhomogeneities. Their magnitude is only a few atomic percents, which is hardly visible by most analytical methods. Still, by using the indicated reference alloy and focussing on differences between adjacent regions, local changes of about 1 at.% could be detected in the present study. Moreover, due to the strong dependence of the transformation start temperature (M_s) on composition in Ni-Al, even small composition variations should result in pronounced structural inhomogeneities. The detected variation of Ni content of about 3at.% can result in a local M_s variation of about 400°C.

These composition inhomogeneities can successfully explain the specific features observed in Ni-Al melt-spun material. In Ni-depleted areas, the local transformation point is too low for transforming B2 into 14M or $L1_0$ at room temperature. In surrounding areas with a slightly higher Ni content, the 14M structure is stable while the $L1_0$ one is stable in areas with the highest Ni-content. The Ni content of the 14M phase was, however, not always measured as intermediate between the $L1_0$ and B2 areas. Probably, the formation of the 14M structure is controlled by both the Ni concentration as well as the local stress configuration existing between the transformed and untransformed regions [9]. The latter can also result in slight changes of twin widths, twin volume fraction, twin plane orientation etc.

As the observed nanoscale composition inhomogeneities are suggested to be the origin for the structural differences in the samples, the appearance of these fluctuations will be discussed. In general it is assumed that the extremely rapid quench does not leave sufficient time for decomposition in the solid state. Thus, the observed compositional variations most probably appear during the crystallisation

process. Crystallisation of binary alloys during conventional casting indeed very often results in spatial redistribution of a solute component. In contrast, rapidly quenched materials usually show the phenomenon of "solute trapping", i.e. solidification without any solute segregation [15]. However, theoretical analysis indicates that in some binary systems freezing a liquid into a solid of the same composition could be thermodynamically impossible. This is particularly the case for systems in which the free energy varies steeply with composition [23,24], which could be the case for Ni-Al alloys with compositions between NiAl and Ni_3Al. If thermodynamic limitation for solute trapping indeed exists in Ni-Al alloys, increasing the quenching rate would only result in a decrease of the characteristic size of the inhomogeneities but not erase compositional variations completely. To our knowledge, the present data provide the first reliable experimental evidence of solute segregation on the nanoscale occurring in materials rapidly quenched from the melt.

5. CONCLUSIONS

Rapidly melt quenched Ni-Al material demonstrates compositional inhomogeneities with a typical size of 500nm and magnitude of a few atomic percents. These inhomogeneities appear most probably during crystallisation and cause broadening of the temperature interval for the $B2 \rightarrow L1_0$ (14M) martensitic transformation. They also lead to a multi-structural state consisting of transformed and untransformed regions. The microstructure of the transformed regions varies from faulted $L1_0$ to faulted 14M.

Acknowledgements

The authors like to thank R. Portier for valuable discussions and suggestions. Pavel Potapov likes to thank the DWTC of the Federal government of Belgium for financial support.

References

1. K.Enami, S.Nenno and K.Shimizu, *Trans.JIM*, **14**, 161 (1973).
2. S. Chakravorty and C.M.Wayman, *Met. Trans. A* , **7A**, 569 (1976).
3. Y.K.Au and C.M.Wayman, *Scr.Metall.*, **6**, 1209 (1972)
4. J.L.Smialek and R.F.Hehemann, *Met. Trans.A*, **A4**, 1571 (1973).
5. F. Renaud, *Scr.Metall.*, **11**, 765 (1977)
6. V.V. Martynov, K.Enami, L.G. Khandros, A.V. Tkachenko and S. Nenno, *Scr. Met.* **17**, 1167. 1983,
7. K.Otsuka, T.Ohba, M.Tokonami and C.M.Wayman, *Scr. Metall. et Mat.*, **29**, 1359 (1993).
8. M.Chandrasekaran and L.Delaey, *J. de Phys.IV*, C4-661 (1982).
9. A.G.Khatchaturyan, S.M.Shapiro and S.Semenovskaya, *Phys.Rev. B*, **43**, 10832 (1991).
10. D. Schryvers and L.E. Tanner, *Trans. MRS Japan 18B*, 849(1993).
11. N.F.Kennon, D.P.Dunne and J.H.Zhu, *J.de Phys.IV*, **5**, C8-1041 (1995).
12. M.Chandrasekaran, J.Beyer and L.Delaey, *Scripta Met.*, **27**, 1841 (1992).
13. D.Schryvers and D.Holland-Moritz, *Intermetallics*, **6**, 427 (1998).
14. P.L.Potapov, P. Ochin, J. Pons and D. Schryvers, to be published.
15. R.W.Cahn, Alloys rapidly solidified from the melt, in "Physical Metallurgy, pp.1780-1852, eds. R.W.Cahn and P.Haansen, North-Holland Physics Publishing, Amsterdam (1983).
16. Y.D.Kim and C.M.Wayman, *Scr.Metall.et Mat.*, **24**, 245 (1990).
17. P.L.Potapov, N.A.Polyakova and V.A.Udovenko, *Scr.Mat.*, **35**, 423 (1996
18. I.M.Robertson and C.M.Wayman, *Phil. Mag.*, **48**, 443 (1983).
19. D.Schryvers and L.E.Tanner, *Ultramicroscopy*, **32**, 241 (1990).
20. Z.Horita, T.Sano and M.Nemoto, *Ultramicroscopy* 21, 271 (1987).
21. D.A.Muller, D.J.Singh and J.Silcox, *Phys.Rev.B*, **57B**, 8181 (1998).
22. G.A.Botton and C.J.Humphreys, *Intermetallics*, **7**, 829 (1999).
23. W.J.Boetinger, Rapidly solidified amorphous and crystalline alloys, *Proc.MRS*, Boston, 15 (1981).
24. R.Mehrabian, *Int. Metallurg. Review*, **27**, 185 (1982).